



Experimental Study of Plasma Actuator Effects on Flow Field Separation Bubble around Blunt Flat Plate

S. Kavousfar¹, E. Esmaeilzadeh^{2†}, H. Mahdavy-Moghaddam³, M. Mirzaei⁴ and S. G. Pouryousefi⁵

^{1,3} Department of Aerospace Engineering, Science and Research Branch, Islamic Azad University, Tehran, Iran

² Heat & Fluid Research Laboratory, Department of Mechanical Engineering, Tabriz University, Tabriz, Iran

^{4,5} Department of Aerospace Engineering, K.N. Toosi University of Technology, Tehran, Iran

†Corresponding Author Email: esmazadeh@tabrizu.ac.ir

(Received November 1, 2014; accepted February 5, 2015)

ABSTRACT

In this paper, the air flow around a blunt flat plate with a rounded leading edge has been experimentally examined with and without the presence of a plasma actuator. Tests have been conducted with Reynolds numbers ranging from 10^4 to 10^5 . Significant phenomena in this flow field is the flow separation at the leading edge of the body, which called separation bubble. There are two considerably dimensionless parameters in this experiment. One of them is the leading edge radius ratio to body thickness and other one is the ratio of maximum velocity induced by plasma actuator to free stream velocity. Geometries with the values of $R/D=0, 1/16, 2/16, 4/16$ were tested. For each geometry, the effectiveness of plasma actuator on the separation bubble is studied in different values of velocity ratio. The results show that, the effect of plasma actuator for the geometry with sharp edge ($R/D=0$), is negligible, while in geometry with rounded edge, the plasma actuator has significant effect on the separation bubble domain. This effectiveness is enhanced, by increasing of leading edge radius and velocity ratio, so that in rounded edge geometry ($R/D=4/16$) length of separation bubble is reduced about 75%.

Keywords: Active flow control, Bluff body; Plasma actuator; Pressure distribution; Reattachment point.

NOMENCLATURE

BR	blockage ratio	P_∞	free stream pressure, Pa
C_f	shear stress coefficient	R	edge radius, m
C_p	pressure coefficient	Re	Reynolds number
D	thickness of the model, m	VR	ratio of maximum velocity of the induced flow to free stream velocity
E	electric field intensity, $\text{kgms}^{-3}\text{A}^{-1}$	V_{PP}	applied voltage (peak to peak), $\text{kgm}^2\text{s}^{-3}\text{A}^{-1}$
F_{ac}	AC-carrier-frequency of the actuator, s^{-1}	V_∞	free stream velocity, ms^{-1}
f_b	body force applied to the particles in the presence of electric field, kgms^{-2}	W	width of the model, m
L	length of the model, m	x_r	location of reattachment point, m
mil	1 mil equals 0.001 inches and 2.54×10^{-5} m	ρ	air density, kgm^{-3}
P	pressure, Pa	ρ_c	electric charge density, sA

1. INTRODUCTION

Control of fluid flow around rigid bodies, particularly the control of boundary layer separation and the forces acting on the body are momentous issues in engineering and technology. Several studies conducted in this case (Artana *et al.* 2001, Braun *et al.* 2009, Brunn and Nitsche 2006, Greenblatt and Wygnanski 2000, Kral 2000). Flow separation from solid surface happens in a different technical applications, such as expanding flow

channels (diffusers), car and train tails and edges, turbomachinery blades and vanes, airfoils at high angles of attack and etc. This perform always leads to a remarkable decrease in efficiency and performance parameters deficiencies (Brunn and Nitsche 2006). The loss of lift, increase of drag and reduction in the pressure recovery are some known effects of separation on the airfoils (Aholt 2009).

The separation bubbles formation in the front part of bluff-bodies has significant importance in

engineering applications. When a fluid flow impacts a bluff-body with sharp edge or when an attached boundary layer faces an adverse pressure gradient with enough magnitude, the flow separation happens, so separation bubble is formed. Separation bubble on the upper surface of an airfoil with the corresponding pressure coefficient distribution is shown in Fig. 1 (O'Meara and Mueller 1987). Downstream the point of separation, illustrated by S, the flow can be almost divided into two main regions. The first region is bounded by the mean dividing streamline ST'R and the body surface. This first region illustrates a slow re-circulatory flow formation of the bubble. The second region of flow encompass the free shear layer limited between the outer edge of the boundary layer S''T''R'' and the dividing streamline. This separated shear layer sustain transition at a location marked by T due to disturbance reinforcement in the unstable laminar layer. Finally, momentum transfer due to turbulent mixing, eliminate the reverse flow near the wall and the flow reattaches at point R. From the beginning of separation point (S) to the point T, pressure is approximately constant on the surface. Then the recovery and increasing of pressure starts and continues until downstream point R (Jahanmiri 2011).

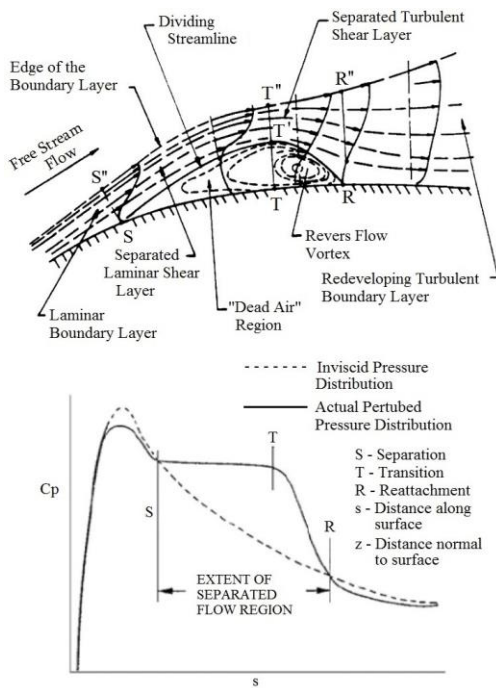


Fig. 1. Separation bubble and distribution of pressure coefficient on surface (O'Meara and Mueller 1987).

Fluid flow around a blunt flat plate and its separation bubble is shown schematically in Fig. 2. After impacting the body, the free stream separates in leading edge and reattaches on surface again. One of the significant parameters in this field is the location of reattachment point on the surface. Flow around a blunt flat plate and its separation bubble have been studied by several people (Kiya and Sasaki 1983, Li and Djilali 1995, Ota *et al.* 1981, Tan *et al.* 2004, Yeung 2004).

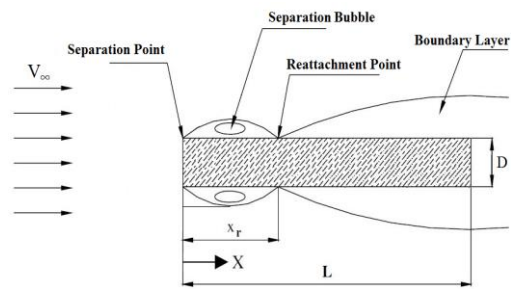


Fig. 2. Schematic structure of the separation bubble in the flow around a blunt flat plate (Yaghoubi and Mahmoodi 2004).

Li and Djilali (1995) conducted an analytical study in the general case of flows having separation bubble with Navier-Stokes equations scaling. The dependency of separation bubble length to Reynolds number in the range of low and moderate Reynolds numbers has been studied and for variations of separation bubble length three state were identified: (i) At low Reynolds numbers, the separation bubble length increases linearly with the Reynolds number (ii) With increasing Reynolds number, the separation bubble length is proportional to the inverse Reynolds number. (iii) At the moderate and higher Reynolds numbers the separation bubble length is constant and independent from the Reynolds number. Yeung (2004) analytically studied pressure distribution of separated reattaching flow in various geometries. Using the experimental results of literatures, relationships have been obtained for pressure distribution of separation bubble in different geometries. In addition to, geometry parameters dependencies and length of reattachment point are investigated.

Presence of bubble has a disruptive effect on the efficiency of equipment. Additionally, separation bubble is sensitive to upstream flow characteristics fluctuations, so that they are prone to instability (Rist and Augustin 2006). This instability consequences in design uncertainty, and has been experimentally perceived to decrease aerodynamic performance as well as result in potentially dangerous dynamic structural loading in aerospace structures (Bak *et al.* 1999; Schreck and Robinson, 2007). Thus, understanding the physics of separation bubble and possible ways to control it, is a necessary precondition for efficient design of aerodynamic devices (Jahanmiri 2011).

To control the size and location of the laminar separation bubble on a FX63-137 airfoil an acoustic source is used by Correa *et al.* (2010). They show that, acoustic actuations are able to decrease the bubble size. Among the active flow control methods, it is shown that the use of plasma actuators in various applications such as flow separation and boundary layer control is effective (Suzen *et al.* 2005). Plasma actuator consists of two electrodes, which are placed on the surface and are separated by a dielectric material, as shown in Fig. 3. An AC high-voltage is applied to the electrodes which causes the surrounding air to be slightly ionized (Tathiri *et al.* 2014). Ionized air is called

plasma and this method of plasma forming is named dielectric barrier discharge (DBD).

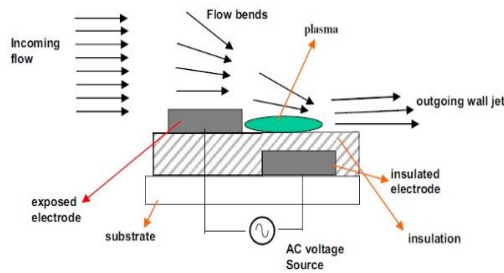


Fig. 3. The structure and arrangement of the electrodes of DBD plasma actuator (Jayaraman and Shyy 2008).

The plasma in presence of the electric field gradient created by the electrodes, results in an effective body force vector on the external flow that can induce steady or unsteady velocity components. This body force can be written in terms of the applied voltage and accommodated to the Navier-Stokes equations. By neglecting magnetic forces, the electrohydrodynamic (EHD) force can be written as (Suzen *et al.* 2005)

$$\vec{f}_b = \rho_c \vec{E} \quad (1)$$

Aerodynamic flow control based on surface DBD Plasma actuator has seen a wonderful growth in penchant in the past 20 years because of its illustrated ability and potential applications. The advantages of DBD Plasma actuator, which is fully electronic with no moving parts, sorely fast response, very low mass and low power consumption (Corke *et al.* 2007). A plasma actuator can be actively controlled, with remarkably immediate response times than are possible via mechanical systems. Thus, a plasma actuator could be designed to respond of varying flow-field conditions, or turned off when it is not necessary (Aholt and Finaish 2011).

The effectiveness of DBD plasma actuators in controlling flow separation has been represented by several researchers. At moderate Reynolds numbers (order of 10^4 to 10^5), the flow field around an airfoil in the presence of plasma actuator has been studied experimentally by Post and Corke (2004). In this research a high angle of attack (8 degrees more than the angle of stall) for the airfoil is chosen, so that the flow separation point is located at the leading edge of the airfoil. They could reduce the flow separation domain and increase ratio of lift to drag approximately 400%. Another applications of plasma actuators, is the flow control of bluff body (circular cylinder) to enhance the aerodynamic performance, which is conducted by Sung *et al.* (2006), Thomas *et al.* (2006) and Do *et al.* (2007). The plasma actuator for noise reduction in bluff body is used by Li *et al.* (2010) and Thomas *et al.* (2008).

Aholt and Finaish (2011) used an active flow control method of separation bubble developed extended over subsonic airfoils at low Reynolds numbers. They made a computational parametric

study to examine the reasonability of an external body force produced by active method, such as a plasma actuator. In this study, the effects of changing the strength and location of the “actuator” on the size and location of the separation bubble and on the aerodynamic performance of the airfoil were illustrated. The body force could effectively omit the separation bubble, when properly located and with sufficient magnitude. Additionally, it was found that by omitting the separation bubble, the aerodynamic efficiency of the airfoil could be enhancing as much as 60%.

The present research is devoted to investigation of DBD plasma actuator effect on separation bubble at leading edge of blunt flat plate with zero angle of attack (Fig. 2). The flow field is studied in Two-dimensions. Therefore, it is necessary for the span of model to be large enough. Due to the body geometry and especially sharp or rounded leading edge effects on the separation bubble, to improve the effectiveness of plasma actuator, rounding of leading edge is used as a combined method. Radius of edge curvature has different values to the body thickness as $R/D=0,1/16,2/16,4/16$. Thus, the effects of two important parameters on the flow field is evaluated (i): DBD plasma actuator, which the maximum velocity induced by DBD to the wind tunnel speed is a dimensionless parameter ($VR=V_{\text{Induced,max}}/V_{\infty}$), (ii): The leading edge curve which relation of its radius to the thickness of the body is also dimensionless parameter of the problem (R/D).

2. EXPERIMENTAL DETAILS

2.1 Wind Tunnel and Model Specification

For experimental setup, a low-speed, open-circuit wind tunnel with a closed wall rectangular test-section of 1.2 m wide, 1 m high, and 3 m long is used (Fig. 4). The longitudinal free-stream turbulence intensity was less than 0.2% and the velocity non-uniformity across the test-section was within $\pm 0.5\%$.



Fig. 4. View of the wind tunnel.

Due to the presence of electric field and the plasma forming on the surface of the body, the model shall be made of insulating material. For this purpose, using a Plexiglas sheet with a thickness of 10 mm, the model is built in the shape of a hollow rectangular cube. The edge of model is also rounded

in required radius. Length of the separation bubble is dependent to free flow conditions and the body geometry. So, for having the reattachment point on the body surface in all experiments conditions, the length of the model is chosen $L=60$ cm. The thickness of the model is $D=8$ cm. In order to achieve the two-dimensional flow, the span of the model was chosen large enough and equal to 90 cm. As it is seen the ratio of model thickness to width of test section (BR) is 0.067 and in the same point of view the ratio of model thickness to model width (D/W) is 0.089. Therefore it is reasonable to accept the symmetry of both side in the measuring region which considered in mid-span of the model. The leading edge radius is variable and for radius values $R=0,5,10,20$ mm, four types of models are built.

According to purpose of this article, which is investigation the Effect of plasma actuator on separation bubble, only one side of the model is selected for installation the electrodes and measuring the pressure. To obtain the surface pressure distribution on the model in separation bubble area, sixty pressure taps of diameter 0.6 mm is furnished within 1 cm distance from each other around the mid-span (symmetry line) of upper surface of the model in a zigzag type. In Fig. 5 the establishment of model in the wind tunnel test section is shown.

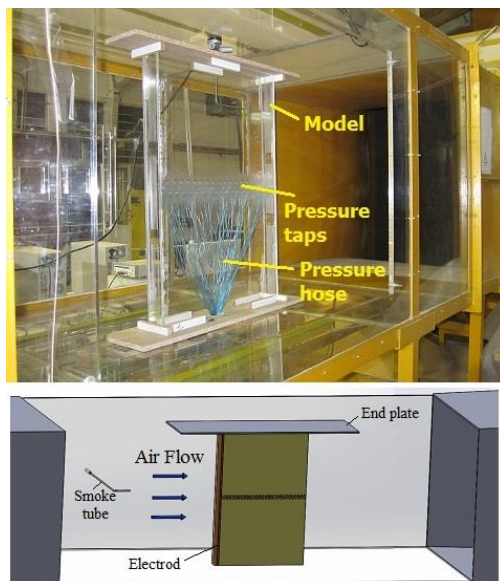


Fig. 5. The establishment of the model in the wind tunnel test section, actual view (top) and schematic (bottom).

The surface pressure measurement system include; pressure transducers (Honeywell-DC005NDC4), a 16 bit- 32 channels National Instruments A/D board (PCI-6224), LabVIEW software, F.S.S (Farasanjesh) PressureField software and a personal computer. The period of each pressure record was 15 s and the sampling rate of 1000 Hz was utilized. In this study, the pressure coefficient C_p , was specified as $C_p = \frac{P - P_\infty}{0.5 \rho_\infty V_\infty^2}$, where P is the average static pressure on the surface of the model, P_∞ , the free-stream static pressure, V_∞ , the free-stream

velocity and ρ_∞ , is the air density. Moreover, the evaluated measurement uncertainty of the mean pressure coefficient is estimated to be at most ± 0.01 .

2.2 Plasma Actuator System

Figure 6 shows a view of the plasma power supply and the electronic measuring system. The plasma power supply that used in the present study was an AC High-Voltage with sinusoidal carrier wave and maximum output electrical power of 1000 W. while the experiments, percentage of the duty cycle and the amplitude of the applied voltage were measured by digital oscilloscope (GW INSTEK GDS-1072-U).



Fig. 6. The external view of the plasma power supply and the electrical measuring devices.

In all the experiments, six layers of 2-mil-thick Kapton polyimide film with the breakdown voltage of almost 7 kV/mil and a dielectric constant of 3.4 were used as the dielectric insulator. Furthermore, the copper planar electrode tapes with a thickness of 50 micron and a length of 45 cm were used. The widths of the exposed and the covered electrodes respectively were 0.5 cm and 1.5 cm, and the overlapping space of electrodes was zero (i.e. edge to edge arrangement).

2.3 Test Conditions in the Wind Tunnel

In all tests the free stream velocity is chosen $V_\infty=5,10,15,20$ m/s. Reynolds number based on the thickness of the model is defined as $Re_D=V_\infty D/v$. For the selective free stream velocities, Reynolds numbers are respectively equal to $Re_D=(2.7,5.4,8.1,10.8)\times 10^4$. For the geometry under study, due to adverse pressure gradients at the sharp leading edge, flow separation occurs exactly in the same area. Thus, for proper effectiveness of the plasma actuator on the separation bubble, location of the electrodes is installed as near as possible to the separation point (Jolibois *et al.* 2008). The electrodes position is schematically depicted in Fig. 7. As seen in Fig. 3, the plasma is formed at the top of insulated electrode and the maximum body force is achieved on the primitive points of this region. So the location of edge to edge of two electrodes is placed at the point of separation beginning. Subsequently, the location of electrodes for geometries with different rounded radius would be

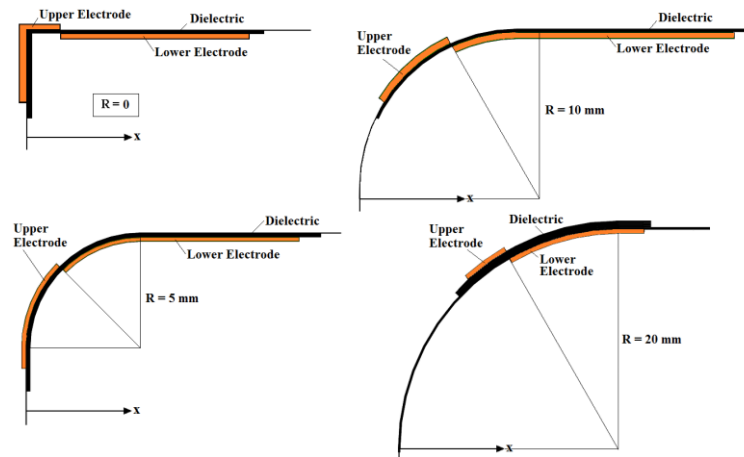


Fig. 7. Schematic of the electrodes position installation.

different. The electrodes position is schematically depicted in Fig. 7. Induced velocity by the plasma actuator is proportional to intensity of applied voltage on the electrodes, as the voltage increases the maximum induced velocity increases too. Maximum induced velocity by the plasma actuator in quiescent air was measured by Pouryoussefi *et al.* (2014). In this reference, a high resolution digital micromanometer and a silicone microtube (0.5 mm diameter) as the Pitot-tube were used for measuring the induced velocity inside the plasma field, where the Pitot-tube was installed downstream the internal edge of the covered electrode with a 5-mm-spacing from this edge and a spacing of 0.5mm from the wall surface. As seen in Fig. 8, maximum effect of plasma actuator is achieved about 5 m/s in voltage intensity of 9 kV. So, the input electrical parameters supplied to the electrodes were applied voltage (V_{PP}) of 9 kV and the carrier frequency (F_{ac}) of 10 kHz. (Pouryoussefi *et al.* 2014).

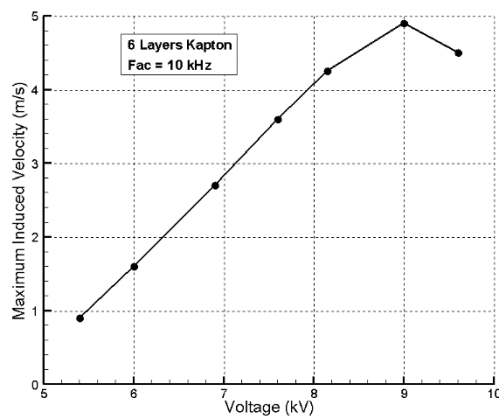


Fig. 8. The maximum velocity induced by plasma actuator vs. applied voltage.

3. PRESSURE DISTRIBUTION AND REATTACHMENT POINT

Average location of the flow reattachment point is considered a point in which the time-averaged shear stress on the wall is equal to zero. Djilali and Gartshore (1991) by measuring the pressure and shear stress distribution on the top surface of blunt

flat plate, obtained the average reattachment point and identified its position in the pressure coefficient diagram at about $x_r=4.7D$. Diagrams of shear stress and pressure coefficient distribution are shown in Fig. 8. Because of flow separation, the pressure on the surface decreases dramatically but inside of the bubble remains constant. Then the pressure recovery is started and in the reattachment region the pressure on the surface increases. The pressure recovery is started from about $x=0.5x_r$ and continued until about $x=1.4x_r$. In another similar study by Suksangpanomrung *et al.* (2000) the range of pressure recovery is about $x=0.375x_r$ to $x=1.35x_r$ and the reattachment point is obtained at $x=4.57D$. This fact can be utilized as a method for using of pressure distribution diagram to identify the location of reattachment point.

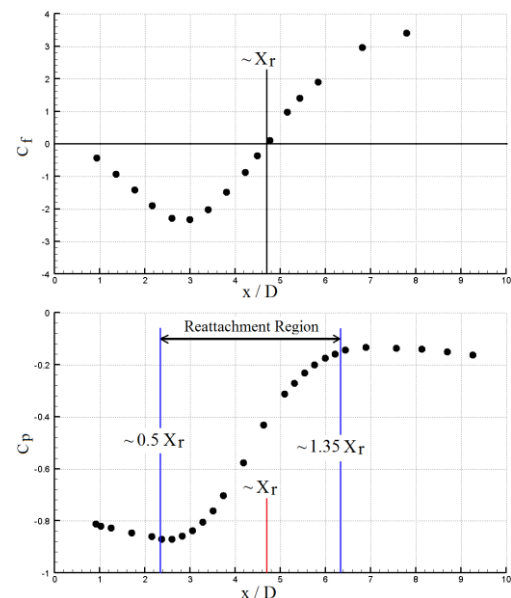


Fig. 9. Distribution of shear stress coefficient (top) and pressure coefficient (bottom) on the surface of the body (Djilali and Gartshore 1991).

4. RESULT AND DISCUSSION

The purpose of this study is to control the separation bubble at the leading edge of the bluff

body by applying force utilizing a DBD plasma actuator. Intensity of flow separation and separation bubble size is a function of the free stream conditions and the geometry of the body. Firstly the test is done on the geometry with sharp corners (no rounded edges). In order to demonstrate the validity and accuracy of measurement and results, the distribution of the pressure coefficient that is obtained in this study is compared with the results provided by Djilali and Gartshore (1991) in Fig. 10.

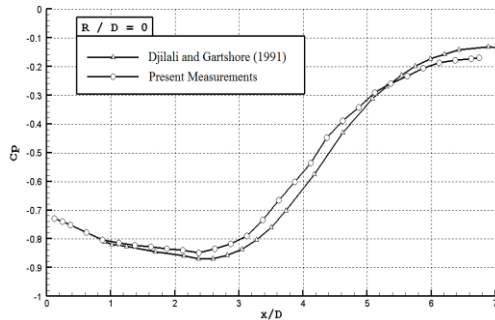


Fig. 10. Comparison of pressure coefficient distribution on the surface of the sharp edge geometry (R/D=0).

Using the criteria given in section 3, for the pressure distribution measured in the present study as shown in Fig. 10, reattachment point position will be $x_r=4.66D$. In another study for $Re=3.6 \times 10^4$ and $AR=4,5,6,9$ by measuring the velocity field using hot wire and calculating shear stress coefficient, the reattachment point is extracted by Yaghoubi and Mahmoodi (2004) which for the same conditions of the present study the reattachment point is $x_r=4.64D$ obtained. The result of present study is compared with other studies with similar conditions which are shown in Table 1. As seen the results of the present study measurements have a reasonable compliance with the references.

Table 1 Comparison of reattachment point positioning with the results of other studies

	$Re_D \times 10^{-4}$	AR	BR(%)	X_r/D
Present Measuremen	2.7-10.8	7.5	6.67	4.66
Djilali and Gartshore (1991)	5	8.89	5.6	4.7
Suksangpanomr ung <i>et al.</i> (2000)	5	12	5.6	4.57
Yaghoubi and Mahmoodi (2004)	3.6	6	4.4	4.5
	3.6	9	4.4	4.75

Distribution of Pressure coefficient for the sharp edge geometry (R/D=0) for velocity ratio of $VR=0,1/4,1/2$ is shown in Fig. 11. For this geometry the results for activated and deactivated plasma, have only slight differences, due to intense gradients at the sharp edge of body, so that the plasma actuator has not enough power to change the structure of this type of flow. Thus, for sharp edge geometry, using a plasma actuator has not changed reattachment point location.

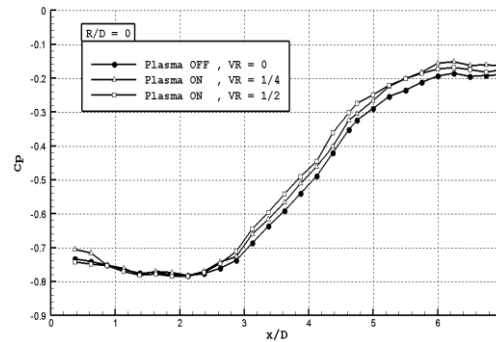


Fig. 11. Distribution of pressure coefficient for sharp-edged geometry (R/D=0) and $V_\infty=10,20$ m/s.

Then, the leading edge is rounded and for various values of the edge radius to thickness ratio ($R/D=1/16,2/16,4/16$), effect of plasma actuator on the separation bubble is studied. Pressure coefficient distribution on geometry of the rounded edge with $R/D=1/16$ and for values of the velocity ratio $VR=0,1/4,1/3,1/2$ is shown in Fig. 12. As seen, by activating the plasma, pressure recovery on the surface occurs sooner than deactivated plasma mode, so that the domain of separation bubble decreases. But because of low quantity of edge radius still, existence gradients are relatively intense. So that plasma actuator effects slightly on the flow structure and bubble domain.

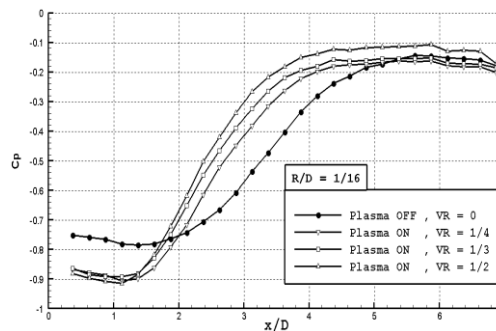


Fig. 12. Distribution of Pressure coefficient for R/D=1/16 in plasma modes on and off.

According to the model given in the previous section (Fig. 9) for determining the location of the reattachment point by using distribution of pressure coefficient, results for $R/D=1/16$ are summarized in Table 2. In this geometry, due to edge roundness, the reattachment point location is 0.85 compared to the sharp edge in the plasma off-mode. By turning on the plasma actuator, the location of this point moves closer to the edge of the body. It is noteworthy that with increasing the free stream velocity and Reynolds number (decreasing VR), the Momentum added to the flow field by the plasma actuator is less than the momentum of main flow, so that the effects of plasma actuator decreases too.

According to the results, it is expected that by increasing of the curve radius at the edge, the intensity and domain of bubble decrease more and effect of plasma actuator to change the flow field structure increases. To do this, the geometry with rounded edge in radius ratio of $R/D=2/16$ is tested.

Table 2 Location of reattachment point for R/D=1/16 in plasma on-mode

V_∞ (m/s)	$Re_D \times 10^{-4}$	VR	1.35 X_r/D	X_r/D	$X_r/(X_r)_{OFF}$	$X_r/(X_r)_{R/D=0}$
10	5.4	1/2	3.875	2.87	0.72	0.61
15	8.1	1/3	4.125	3.06	0.77	0.65
20	10.8	1/4	4.375	3.24	0.81	0.69
Plasma OFF	0		5.375	3.98	1.00	0.85

Table 3 Location of reattachment point for R/D=2/16 in plasma on-mode

V_∞ (m/s)	$Re_D \times 10^{-4}$	VR	1.35 X_r/D	X_r/D	$X_r/(X_r)_{OFF}$	$X_r/(X_r)_{R/D=0}$
5	2.7	1	2	1.48	0.50	0.32
10	5.4	1/2	2.5	1.85	0.63	0.39
15	8.1	1/3	3.25	2.41	0.81	0.51
20	10.8	1/4	3.5	2.59	0.88	0.55
Plasma OFF	0	4	2.96	1.00	0.63	

In this geometry for the free stream velocity in addition to the previous quantities, amount of 5 m/s has been tested. Distribution of pressure Coefficient on the surface of the body is shown in Fig. 13. According to these diagrams, for the free stream velocity 5 m/s, plasma actuator has been able to significantly alter the pressure distribution; subsequently the separation bubble domain is also greatly reduced. By increasing free stream velocity to $V_\infty=10$ m/s, effect of plasma actuator is slightly reduced. In these conditions, relatively small bubble is formed. With further increase for free stream velocity and subsequently reduction of VR, again like the previous geometry, the plasma actuator effectiveness is limited. As for the free stream velocity $V_\infty=15$ m/s and $V_\infty=20$ m/s plasma actuator has less effect on the separation bubble and pressure recovery on the reattachment region.

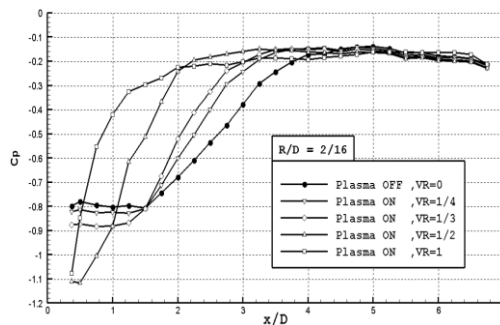


Fig. 13. Pressure coefficient distribution for R/D=2/16 in plasma on-mode and off-mode.

The location of reattachment point in the plasma on-mode for R/D=2/16 is summarized in Table 3. As expected for this geometry, plasma actuator has a strong effect on fluid flow and separation bubble, in the way that length of reattachment point has

significant reposition compared to the previous geometry. In this geometry, the effect of roundness edge reduces length of separation bubble about 37% which by adding effect of plasma actuator, this reduction enhances to the 68% (in state of VR=1).

In continues, the radius of edge would increase to R/D=4/16. The results are shown in Fig. 14. For free stream velocity of 5 m/s and 10 m/s by applying plasma actuators, pressure recovery was greatly impressed. In fact, in these conditions, separation bubble is almost gone. Due to flow path rotation around the rounded edge, the pressure reduces, then immediately the pressure is recovered. In The free stream velocity of 15 m/s, the length of separation bubble is very small too. But with increasing free stream velocity to 20 m/s again the intensity of plasma actuator compared to the free stream momentum decreases and its effect on the fluid flow is negligible.

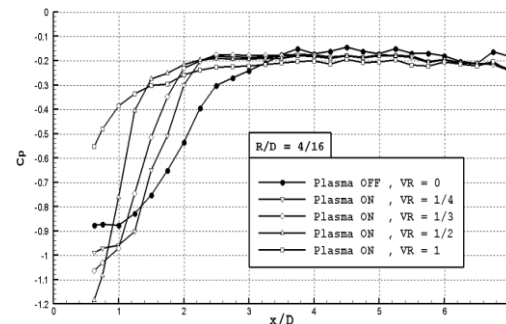


Fig. 14. Pressure coefficient distribution for R/D=4/16 in plasma on-mode and off-mode.

Results of reattachment point location for the geometry of R/D=4/16 is summarized in Table 4. In this geometry, the effect of edge roundness which is

Table 4 Location of reattachment point for R/D=4/16 in plasma on-mode .

V_∞ (m/s)	$Re_D \times 10^{-4}$	VR	1.35 X_r/D	X_r/D	$X_r/(X_r)_{OFF}$	$X_r/(X_r)_{R/D=0}$
5	2.7	1	1.5	1.11	0.46	0.24
10	5.4	1/2	1.75	1.30	0.54	0.28
15	8.1	1/3	2	1.48	0.62	0.32
20	10.8	1/4	2.25	1.67	0.69	0.35
Plasma OFF		0	3.25	2.41	1.00	0.51

reduced location of reattachment point as much as 49 percent. Also, by adding the effect of the plasma actuator, length of the separation bubble is approximately 76% (at VR=1) is reduced in comparison to the sharp edge geometry.

To exhibit the effect of the plasma actuator on separation bubble domain, a case of conducted experiments is visualized by using of the smoke injection technique. For this purpose the geometry with a radius of R/D=4/16 at the free stream velocity 5 m/s is selected due to its highest change in separation bubble. Using a video camera installed at the position shown in Fig. 5, the photography of this process was done. Visualization of flow is shown in both plasma on and off mode in Fig. 15. It can be seen that the separation bubble domain affected by the plasma actuator is significantly decreased, which is compatible with the results of the distribution of pressure coefficient.

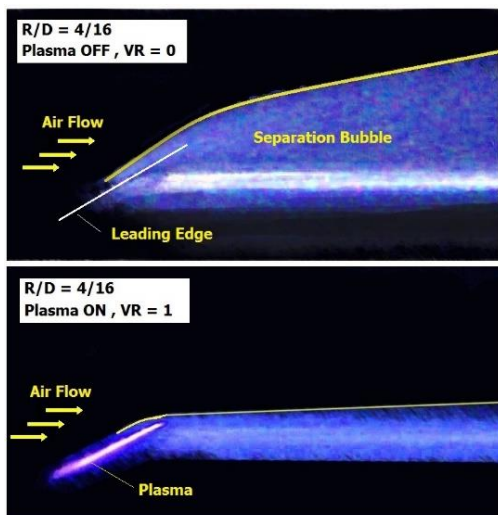


Fig. 15. Visualization of flow field in the both plasma off-mode (top) and on-mode (bottom) for R/D=4/16 and $V_\infty=10$ m/s.

5. CONCLUSION

In this paper, the flow field around a bluff body with and without the presence of plasma actuator was tested. The effect of the plasma actuator on the rounded edge geometry for different radii was determined. Both dimensionless parameter R/D and VR are effective on change of separation bubble

length. It was observed that in sharp edge geometry (R/D=0) due to intensive adverse pressure gradient and stronger separation bubble formation, effect of plasma is not significant. By increasing the radius of the rounded leading edge, adverse pressure gradient is reduced and plasma actuator has better effect to develop changes in the structure of the separation bubble. In addition to, in low Reynolds number the added momentum to flow field by the plasma actuator relative to the free stream momentum has considerable value and effects significantly better. This issue is identified by a dimensionless parameter VR, which for a specified geometry by increasing the free stream velocity and reduction of VR also the effect of plasma actuator is reduced. So for formation of smaller separation bubble, it is needed to use a geometry with a larger radius ratio and the larger velocity ratio (VR). The obtained results showed that in the case of R/D=4/16 with $Re=2.7 \times 10^4$ and VR=1 separation bubble almost disappears. If we could increase the intensity of the plasma actuator (which requires the design of a new plasma actuator system) separation bubble size can be reduced in geometries having stronger pressure gradient.

REFERENCES

- Aholt, J. (2009). Influence of Laminar Separation Bubbles on the Aerodynamic Characteristics of Elliptical Airfoils at Low Reynolds Numbers. *2008-2009 Missouri Space Grant Consortium Student Reports and Abstracts*, MOSGC, Columbia, MO.
- Aholt, J. and F. Finaish (2011). Active Flow Control Strategy of Laminar Separation Bubbles Developed over Subsonic Airfoils at Low Reynolds Numbers. *AIAA Paper* 2011-733.
- Artana, G., J. D'Adamo, L. Léger, E. Moreau and G. Touchard (2001). Flow Control with Electrohydrodynamic Actuators. *AIAA Paper* 2001-0351.
- Bak, C., H. A. Madsen, P. Fuglsang and F. Rasmussen (1999). Observations and Hypothesis of Double Stall. *Wind Energy* 2(1), 195–210.
- Braun, E. M., F. K. Lu and D. R. Wilson (2009).

- Experimental research in aerodynamic control with electric and electromagnetic fields. *Progress in Aerospace Sciences* 45, 30-49.
- Brunn, A. and W. Nitsche (2006). Active control of turbulent separated flows over slanted surfaces. *International Journal of Heat and Fluid Flow* 27, 748-755.
- Corke, T. C., M. L. Post and D. M. Orlov (2007). SDBD plasma enhanced aerodynamics: concepts, optimization and applications. *Progress in Aerospace Sciences* 43, 193-217.
- Correa, L. G. N., R. M. U. Entz, R. Cosin and F. M. Catalano (2010). Acoustic Control of Laminar Separation Bubble. *27th International Congress of the Aeronautical Sciences (ICAS 2010)*, Nice, France.
- Djilali, N. and I. S. Gartshore (1991). Turbulent flow around a bluff rectangular plate. Part I: Experimental investigation. *ASME J. Fluids Eng.* 113, 51-59.
- Do, H., W. Kim, M. G. Mungal and M. A. Cappelli (2007). Bluff Body Flow Separation Control using Surface Dielectric Barrier Discharges. *AIAA Paper* 2007-939.
- Greenblatt, D. and I. J. Wagnanski (2000). The control of flow separation by periodic excitation. *Progress in Aerospace Sciences* 36, 487-545.
- Jahanmiri, M. (2011). Laminar Separation Bubble: Its Structure, Dynamics and Control. *Research report* 2011:06, Dept. of Applied Mechanics, Chalmers University of Technology, Sweden.
- Jayaraman, B. and W. Shyy (2008). Modeling of dielectric barrier discharge-induced fluid dynamics and heat transfer. *Progress in Aerospace Sciences* 44, 139-191.
- Jolibois, J., M. Forte and E. Moreau (2008). Application of an AC barrier discharge actuator to control airflow separation above a NACA 0015 airfoil: Optimization of the actuation location along the chord. *Journal of Electrostatics* 66, 496-503.
- Kiya, M. and K. Sasaki (1983). Structure of a turbulent separation bubble. *J. Fluid Mech.* 137, 83-113.
- Kral, L. D. (2000). Active Flow Control Technology. *ASME Fluids Engineering Technical Brief*.
- Li, X. and N. Djilali (1995). On the Scaling of Separation Bubbles. *JSME International Journal, Series B* 38(4), 541-548.
- Li, Y., X. Zhang and X. Huang (2010). The use of plasma actuators for bluff body broadband noise control. *Experiments in Fluids* 49(2), 367-377.
- O'Meara, M. M. and T. J. Mueller (1987). Laminar Separation Bubble Characteristics on an Airfoil at Low Reynolds Numbers. *AIAA Journal*, 25(8), 1033-1041.
- Ota, T., Y. Asano and J. I. Okawa (1981). Reattachment length and transition of the separated flow over blunt flat plates. *Bulletin of the JSME* 24(192), 941-947.
- Post, M. L. and T. C. Corke (2004). Separation Control on a High Angle of Attack Airfoil Using Plasma Actuators. *AIAA Journal* 42(11), 2177-2184.
- Pouryoussefi, S. G., M. Mirzaei and M. Hajipour (2014). Experimental study of separation bubble control behind a backward-facing step using plasma actuators. *Acta Mechanica*, Published online: 07 October 14-1245-7.
- Rist, U. and K. Augustin (2006). Control of Laminar Separation Bubbles Using Instability Waves. *AIAA Journal* 44(10), 2217-2223.
- Schreck, S. J. and M. C. Robinson (2007). Horizontal Axis Wind Turbine Blade Aerodynamics in Experiments and Modeling. *IEEE Transactions on Energy Conversion* 22(1), 61-70.
- Suksangpanomrung, A., N. Djilali and P. Moinat (2000). Large-eddy simulation of separated flow over a bluff rectangular plate. *International Journal of Heat and Fluid Flow* 21, 655-663.
- Sung, Y., W. Kim, M. G. Mungal and M. A. Cappelli (2006). Aerodynamic Modification of Flow over Bluff Objects by Plasma Actuation. *Experiments in Fluids* 41(3), 479-486.
- Suzen, Y. B., P. G. Huang, J. D. Jacob and D. E. Ashpis (2005). Numerical simulations of plasma based flow control applications. *AIAA Paper* 2005-4633.
- Tan, B. T., M. C. Thompson and K. Hourigan (2004). Flow past rectangular cylinders: receptivity to transverse forcing. *J. Fluid Mech.* 515, 33-62.
- Tathiri, G., E. Esmaeilzadeh, S. M. Mirsajedi and H. Mahdavi Moghaddam (2014). Experimental Investigation of Why an AC Dielectric Barrier Discharge Plasma Actuator is Preferred to DC Corona Wind Actuator in Boundary Layer Flow Control *Journal of Applied Fluid Mechanics* 7(3), 525-534.
- Thomas, F. O., A. Kozlov and T. C. Corke (2006). Plasma Actuators for Bluff Body Flow Control. *AIAA Paper* 2006-2845.
- Thomas, F. O., A. Kozlov and T. C. Corke (2008). Plasma Actuators for Cylinder Flow Control and Noise Reduction. *AIAA Journal* 46(8),

S. Kavousfar *et al.* / *JAFM*, Vol. 9, No. 1, pp. 397-406, 2016.

1921-1931.

105-112.

Yaghoubi, M. and S. Mahmoodi (2004).
Experimental study of turbulent separated and
reattached flow over a finite blunt plate.
Experimental Thermal and Fluid Science 29,

Yeung, W. W. H. (2004). Analysis and modeling of
pressure induced by separated reattaching flows.
24th international congress of the aeronautical
sciences.